Driving Force Dependence of Photoinduced Electron Transfer Dynamics of Intercalated Molecules in DNA

Shunichi Fukuzumi,*,† Mari Nishimine,† Kei Ohkubo,† Nikolai V. Tkachenko,‡ and Helge Lemmetyinen*,‡

Department of Material and Life Science, Graduate School of Engineering, CREST, Japan Science and Technology Agency, Osaka University, Suita, Osaka 565-0871, Japan, and The Institute of Materials Chemistry, Tampere University of Technology, P.O. Box 541, FIN-33101 Tampere, Finland

Received: April 16, 2003; In Final Form: September 12, 2003

A series of acridinium, quinolinium, and phenanthridinium ions (9-substituted-10-methylacridinium ($AcrR^+$, R = H, Pr^i, and CH_2Ph), 3-substituted-1-methylquinolinium ($RQuH^+$, R = CN and Br), and 5-methylphenanthridinium (5-$MePhen^+$) perchlorate salts) are shown to be intercalated into the DNA double helix from calf thymus. The one-electron reduction potentials (E^0_{red}) of these intercalators have been determined in the absence and presence of DNA by both cyclic voltammetry and second harmonic ac voltammetry. The E^0_{red} values of intercalators are shifted in a positive direction by intercalation into the DNA double helix. The one-electron oxidation potential (E^0_{ox}) of ethidium bromide, which is known to be intercalated into DNA, is also shifted in a positive direction by the intercalation. The wide range of E^0_{red} values of intercalators thus determined in the presence of DNA allows us to examine the exact driving force dependence of the rates of photoinduced electron transfer from the singlet excited state of ethidium bromide to the intercalators in DNA for the first time. The resulting data were evaluated in light of the Marcus theory of electron transfer to determine the reorganization energy and the electron coupling matrix element in DNA.

Introduction

Photoinduced electron transfer (PET) in DNA has been a topic of significant interest in recent years because of a crucial role in photochemical reactions leading to the oxidative damage of DNA.[1−10] Synthetic fluorescent dyes such as ethidium bromide readily intercalate into the DNA double helix, and they are widely used as a tool to study PET dynamics in DNA.[9−13] Extensive studies have been focused on the distance dependence of PET dynamics in DNA.[1,3−8,14,15] The driving force dependence of PET in DNA has also merited special attention in light of the Marcus theory of electron transfer.[3,16] The redox potential of an intercalated molecule is expected to be altered by intercalation because the environment is changed from an aqueous phase to a space between π-stacked nucleobase pairs. However, only small changes in the redox potentials of intercalators in the presence of DNA have so far been reported in the pulse radiolysis studies.[17] There has been no systematic electrochemical study on the change in the redox potentials of intercalators associated with the intercalation into DNA. In addition, the lack of appropriate intercalators having a wide range of redox potentials has precluded a detailed investigation of the driving force dependence of PET of intercalated molecules in DNA.

We report herein the driving force dependence of the PET dynamics of 9-substituted-10-methylacridinium ion ($AcrR^+$, R = H, Pr^i, and CH_2Ph), 3-substituted-1-methyl-quinolinium ion ($RQuH^+$, R = CN and Br), and 5-methylphenanthridinium ion (5-$MePhen^+$) perchlorate salts, which can readily intercalate into the DNA double helix from calf thymus. Such a series of intercalators enable us to cover a wide range of the driving force of PET from the singlet excited state of ethidium bromide in DNA. The driving force of PET in DNA, being different from that in an aqueous solution, has been determined experimentally for the first time from the redox potentials of intercalators, which are indeed altered significantly by intercalation into DNA.

Experimental Section

Materials. Ethidium bromide (Eth^+Br^-) and calf thymus deoxyribonucleic acid sodium salt (DNA) were purchased from Sigma Chemical Co. A stock solution of DNA (18 mg in 25 mL of solvent) was prepared by dissolution overnight in 5 mM Tris-HCl buffer (pH 7.0) containing 5 mM sodium sulfate (Na_2SO_4). Tris(hydroxymethyl)aminomethane was purchased from Nacalai Tesque, Japan. *p*-Benzoquinone, methyl-*p*-benzoquinone, hydrochloric acid, and sodium sulfate (99.9%) were purchased from Wako Pure Chemical Ind. Ltd., Japan. Chloro-*p*-benzoquinone was purchased from Aldrich. 10-Methylacridinium iodide was prepared by the reaction of acridine with methyl iodide in acetone, converted to the perchlorate salt ($AcrH^+ClO_4^-$) by the addition of $Mg(ClO_4)_2$ to the iodide salt, and purified by recrystallization from methanol.[18,19] 9-Substituted 10-methylacridinium perchlorates ($AcrR^+ClO_4^-$: R = Pr^i and CH_2Ph) were prepared by the reaction of 10-methylacridone in dichloromethane with the corresponding Grignard reagents (RMgBr), followed by the addition of sodium hydroxide for the hydrolysis and perchloric acid for the neutralization, and were purified by recrystallization from ethanol−diethyl ether.[20]

* To whom correspondence should be addressed. S.F. E-mail: fukuzumi@ap.chem.eng.osaka-u.ac.jp. Fax: +81-6-6879-7370. H.L. E-mail: lemme@cc.tut.fi.

† Osaka University.

‡ Tampere University of Technology.

10.1021/jp035023p CCC: $25.00
Published on Web 10/18/2003

1-Methylquinolinium perchlorate ($QuH^+ClO_4^-$), 3-bromo-1-methylquinolinium perchlorate ($BrQuH^+ClO_4^-$), 3-cyano-1-methylquinolinium perchlorate ($CNQuH^+ClO_4^-$), and 5-methylphenanthridinium perchlorate (5-$MePhen^+ClO_4^-$) were prepared by the reaction of the corresponding quinoline derivatives with methyl iodide in acetone, followed by metathesis with $Mg(ClO_4)_2$.[20] The purity of synthesized intercalators was checked by elemental analysis and ^1H NMR (300 MHz). $AcrPr^{i+}ClO_4^-$: ^1H NMR (CD_3CN): δ 1.82 (d, 6H $J = 7.8$ Hz), 4.72(s, 3H) 4.79 (m, 1H, $J = 7.8$ Hz), 7.94 (t, 2H, $J = 7.8$ Hz), 8.34 (t, 2H, $J = 7.8$ Hz), 8.53 (d, 2H, $J = 7.8$ Hz), 8.92 (d, 2H, $J = 7.8$ Hz). Anal. Calcd for $C_{17}H_{18}NO_4Cl$: C, 60.81; H, 5.40; N, 4.17. Found: C, 61.32; H, 5.39; N, 4.17. $AcrCH_2Ph^+ClO_4^-$: ^1H NMR (CD_3CN): δ 4.79 (s, 3H), 5.35 (s, 2H), 7.5−8.9 (m, 13H). Anal. Calcd for $C_{21}H_{18}NO_4Cl$: C,65.71; H, 4.73; N, 3.65. Found: C, 65.29; H, 4.66; N, 3.67. $BrQuH^+ClO_4^-$: ^1H NMR (CD_3CN): δ 4.56 (s, 3H), 8.07 (t, 2H, $J = 8.3$ Hz), 8.2−8.4 (m, 4H). Anal. Calcd for $C_{10}H_9NO_4BrCl\cdot H_2O$: C, 35.27; H, 3.26; N, 4.11. Found: C, 34.97; H, 2.77; N, 4.05. $CNQuH^+ClO_4^-$: ^1H NMR (CD_3CN): δ 4.61 (s, 3H), 8.12−8.24 (m, 1H), 8.4−8.5 (m, 3H), 9.46 (s, 1H), 9.52 (s, 1H). Anal. Calcd for $C_{11}H_9N_2O_4Cl$: C, 49.18; H, 3.38; N, 10.43. Found: C, 49.01; H, 3.30; N, 10.58. 5-$MePhen^+ClO_4^-$: ^1H NMR (CD_3CN): δ 4.63 (s, 3H), 8.0−8.6 (m, 6H), 8.8−9.2 (m, 2H), 9.77 (s, 2H). Anal. Calcd for $C_{14}H_{12}NO_4Cl$: C, 57.25; H, 4.12; N, 4.77. Found: C, 57.15; H, 4.06; N, 4.72. Water was purified (18.3 MΩ cm) with a Milli-Q system (Millipore; Milli-Q Jr.). Acetonitrile was purified and dried by the standard procedure.[21]

Electrochemical Measurements. Cyclic voltammetry (CV) and second-harmonic ac voltammetry (SHACV)[22] measurements were performed at 298 K on a BAS 100W or BAS 100B electrochemical analyzer in deaerated Tris-HCl buffer containing 5 mM Na_2SO_4 as the supporting electrolyte. A conventional three-electrode cell was used with a gold working electrode (surface area of 0.3 mm^2) and a platinum wire as the counter-electrode. The gold working electrode (BAS) was polished with BAS polishing alumina suspension and rinsed with acetone before use. The reference electrode was Ag/0.01 M AgCl. The values (vs Ag/AgCl) are converted to those versus SCE by adding 0.04 V.[23]

Spectroscopic Measurements. Changes in the UV−vis spectra of several substrates were monitored by using a Hewlett-Packard 8452A diode array spectrophotometer. The interaction between intercalators and DNA was examined from the change in the UV−vis spectra of intercalators in the presence of various concentrations of DNA ($0-2.0 \times 10^{-3}$ M). Concentration of DNA per nucleobase was estimated using $\epsilon = 6600\ M^{-1}\ cm^{-1}$ at 260 nm.[24]

Quenching experiments of the fluorescence of Eth^+ were carried out on Shimadzu RF-5000 and RF-5300PC spectrofluorophotometers. The excitation energy of $^1Eth^{+*}$ in DNA is determined from the absorption and fluorescence maxima to be 2.24 eV, which is lower than that in H_2O (2.33 eV). The excitation wavelengths of Eth^+ in the presence of DNA (1.4×10^{-3} M) and in the absence of DNA in 5 mM Tris-HCl buffer were 520 and 480 nm, respectively. The monitoring wavelengths were those corresponding to the maxima of the emission band of 591 and 598 nm, at which there is no absorption because of a quencher and thus no inner filter effects on the fluorescence quenching are observed. The buffer solutions were deaerated by argon purging for 10 min prior to the measurements. Relative fluorescence intensities were measured for buffer solutions containing Eth^+ (5.0×10^{-5} M) with a quencher at various concentrations ($0-3.0 \times 10^{-3}$ M) in the presence of DNA (1.5×10^{-3} M). There was no change in the shape, but there was a change in the intensity of the fluorescence spectrum by the addition of a quencher.

CHART 1

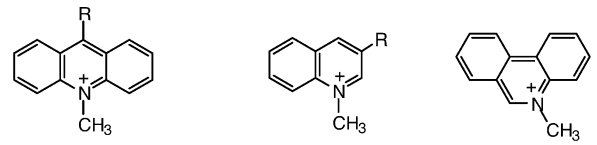

$AcrR^+$ (R = H, Pr^i, CH_2Ph,) $RQuH^+$ (R = CN, Br) 5-$MePhen^+$

Time-resolved fluorescence spectra were measured by a Photon Technology International GL-3300 with a Photon Technology International GL-302 and a nitrogen laser/pumped dye laser system equipped with a four-channel digital delay/pulse generator (Stanford Research System Inc. DG535) and a motor driver (Photon Technology International MD-5020). The excitation wavelength was 520 nm using coumarin 540A (Exciton Co.) as a dye. Fluorescence lifetimes were determined by a two-exponential curve fit using a microcomputer. Nanosecond transient absorption measurements were carried out using a Nd:YAG laser (Solar, TII) at 532 nm with a power of 60 mJ as an excitation source. The transient spectra were recorded using fresh solutions in each laser excitation. All experiments were performed at 298 K.

Results and Discussion

Change in One-Electron Redox Potentials of Intercalators in DNA. The intercalators employed in this study are shown in Chart 1. The changes in the one-electron reduction potentials of intercalators were examined by the cyclic voltammetry (CV) and second-harmonic ac voltammetry (SHACV) measurements.[22,25] A typical example is shown in Figure 1. A quasi-reversible CV wave is observed for the one-electron redox couple of $AcrPr^{i+}/AcrPr^{i\bullet}$ in deaerated 5 mM Tris-HCl buffer aqueous solution at a sweep rate of 0.01 V s^{-1} (Figure 1a). The half-wave potential is determined to be −0.70 V (vs SCE), which remains the same at different sweep rates. The CV half-wave potential (Figure 1a) agrees with the SHACV intersection potential (Figure 1b), and this value is taken as the one-electron reduction potential (E^0_{red}) of $AcrPr^{i+}$. The E^0_{red} value of $AcrPr^{i+}$ in an aqueous solution is more negative as compared to the value (−0.63 V) in acetonitrile (MeCN)[20] because of the stronger solvation of $AcrPr^{i+}$ in water than in MeCN. In the presence of DNA (2.0×10^{-3} M), the one-electron reduction potential of $AcrPr^{i+}$ is shifted in a positive direction, exhibiting a quasi-reversible wave at −0.56 V (vs SCE) as shown in Figure 1c. Figure 1d shows the corresponding SHACV in which the E^0_{red} value is determined from the intersection potential of two curves of opposite phases as −0.56 V, which agrees with the value from the CV (Figure 1c). The change in the E^0_{red} value as a function of the ratio of the DNA concentration to the initial concentration of $AcrPr^{i+}$, [DNA bases]/$[AcrPr^{i+}]_0$, is shown in Figure 2a, where the data from CV and SHACV agree with each other. The E^0_{red} value increases with increasing DNA concentration to approach a constant value in the region of [DNA bases]/$[AcrPr^{i+}]_0 > 30$, although the higher DNA concentration ($> 2.0 \times 10^{-3}$ M) is limited by the solubility

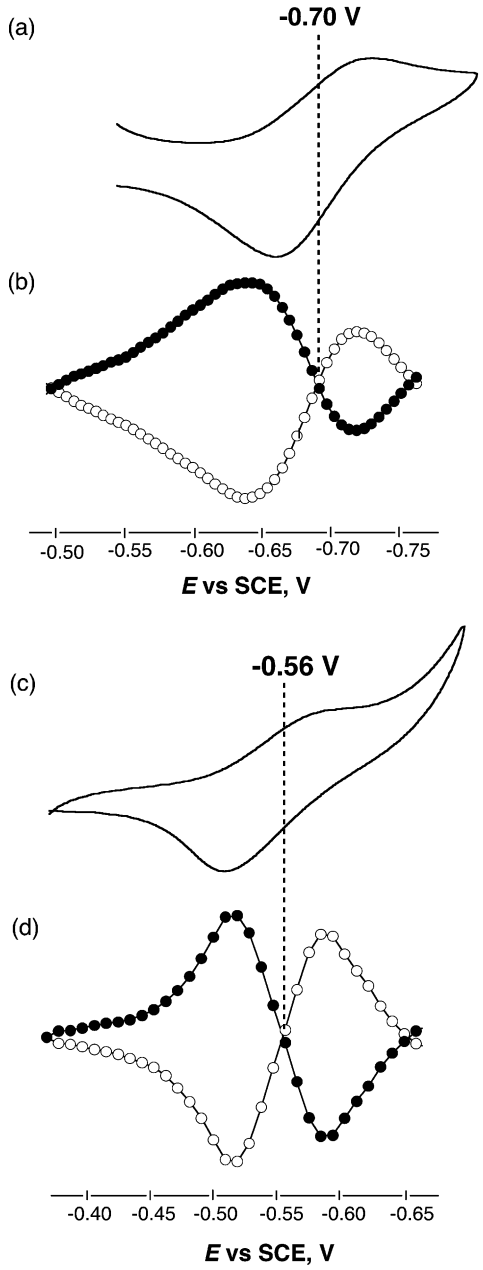

Figure 1. (a) Cyclic voltammogram (sweep rate of 10 mV s^{-1}) and (b) second-harmonic ac voltammogram (sweep rate of 4 mV s^{-1}) of $AcrPr^{i+}$ (5.0×10^{-4} M) in 5 mM Tris-HCl buffer (pH 7.0). (c) Cyclic voltammogram (sweep rate of 10 mV s^{-1}) and (d) second-harmonic ac voltammogram (sweep rate of 4 mV s^{-1}) of $AcrPr^{i+}$ (5.0×10^{-5} M) in the presence of DNA (2.0×10^{-3} M) in 5 mM Tris-HCl buffer (pH 7.0).

problem. This indicates that the change in E^0_{red} is attributed to the intercalation of $AcrPr^{i+}$ into DNA.

A bathchromic shift and the hypochromicity of its visible absorption band is observed in the electronic absorption spectrum of $AcrPr^{i+}$ in the presence of DNA in deaerated 5 mM Tris-HCl buffer as compared to that in the absence of DNA. The ratio of the intercalated $AcrPr^{i+}$ molecules is obtained from the absorbance change of $AcrPr^{i+}$ with DNA concentration by using eq 1, where [DNA bases−$AcrPr^{i+}$] and $[AcrPr^{i+}]_0$ are the concentrations of the intercalated $AcrPr^{i+}$ and the initial concentration of $AcrPr^{i+}$ and A_0, A, and A_∞ are the initial absorbances in the absence of DNA, at a given concentration of DNA, and at a large concentration of DNA when all $AcrPr^{i+}$ molecules are intercalated into DNA, respectively. The binding

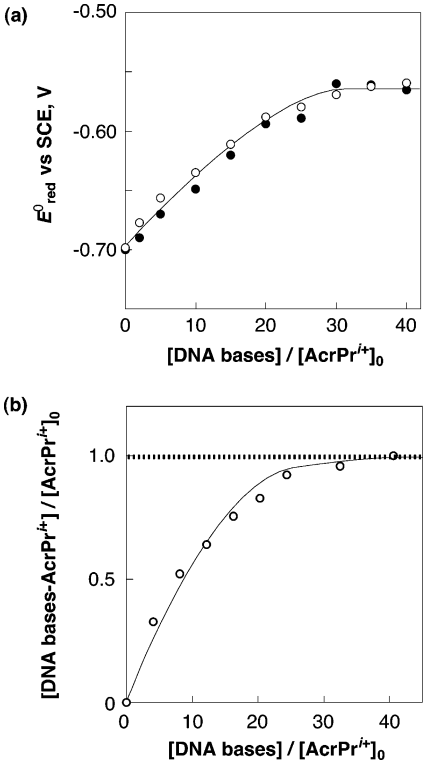

Figure 2. (a) Plot of the one-electron reduction potential of $AcrPr^{i+}$ (5.0×10^{-5} M) vs the ratio of the concentration of DNA bases (0−2.0 $\times 10^{-3}$ M) to $AcrPr^{i+}$ in 5 mM Tris-HCl buffer (pH 7.0), determined by CV (○) and SHACV (●). (b) Plot of the ratio of intercalated $AcrPr^{i+}$ (5.0×10^{-5} M) vs the concentration of DNA (0−2.0×10^{-3} M) to $AcrPr^{i+}$.

constant (K) of $AcrPr^{i+}$ with DNA is given by eq 2.

$$\frac{[\text{DNA bases}-\text{AcrPr}^{i+}]}{[\text{AcrPr}^{i+}]_0} = \frac{(A_0 - A)}{(A_0 - A_\infty)} \tag{1}$$

$$K = \frac{[\text{DNA bases}-\text{AcrPr}^{i+}]}{([\text{AcrPr}^{i+}]_0 - [\text{DNA bases}-\text{AcrPr}^{i+}])([\text{DNA}]_0 - [\text{DNA bases}-\text{AcrPr}^{i+}])} \tag{2}$$

The plot of [DNA bases−$AcrPr^{i+}$]/$[AcrPr^{i+}]_0$ versus [DNA bases]/$[AcrPr^{i+}]_0$ determined from the absorbance change (eq 1) is shown in Figure 2b. The [DNA bases−$AcrPr^{i+}$]/$[AcrPr^{i+}]_0$ value increases with an increase in the [DNA bases]/$[AcrPr^{i+}]_0$ value to reach a constant value in the region of [DNA bases]/$[AcrPr^{i+}]_0 > 30$, where all $AcrPr^{i+}$ molecules are intercalated into DNA. The binding constant K is determined to be 2.0×10^3 M^{-1} from the data in Figure 2b using eq 2. The binding constant is readily estimated as [DNA bases]$^{-1}$, which gives the ratio of [DNA bases−$AcrPr^{i+}$]/$[AcrPr^{i+}]_0 = 0.5$. The change in the E^0_{red} value with [DNA bases]/$[AcrPr^{i+}]_0$ in Figure 2a is in parallel agreement with that in [DNA bases$AcrPr^{i+}$]/[Acr-$Pr^{i+}]_0$ in Figure 2b. Such a parallel relationship clearly indicates that the potential shift of E^0_{red} of $AcrPr^{i+}$ is caused by the intercalation of $AcrPr^{i+}$ into DNA. Because the E^0_{red} value is shifted in a positive direction, the $AcrPr^{i\bullet}$ radical produced by the one-electron reduction of $AcrPr^{i+}$ may be more stabilized by the $\pi-\pi$ interaction with base pairs of DNA as compared to that in an aqueous buffer solution. The solvation of water to $AcrPr^{i+}$ also plays an important role in determining the E^0_{red} value because the E^0_{red} value is known to be shifted in a positive

TABLE 1: One-Electron Reduction Potentials (E^0_{red}) of Intercalators in the Presence of DNA (2.0×10^{-3} M) and in the Absence of DNA and Driving Force ($-\Delta G^0_{ET}$) and Rate Constants (k_{ET}) of Photoinduced Electron Transfer

no	intercalator	E^0_{red} vs SCE, V[a]	$-\Delta G^0_{ET}$, eV	k_{ET}, s^{-1}
1	$AcrH^+$	−0.11 (−0.30)	0.67	4.3×10^8
2	$AcrCH_2Ph^+$	−0.45 (−0.48)	0.33	1.3×10^9
3	$AcrPr^{i+}$	−0.56 (−0.70)	0.22	4.6×10^8
4	$CNQuH^+$	−0.60 (−0.79)	0.18	1.8×10^8
5	$BrQuH^+$	−0.76 (−0.82)	0.02	9.6×10^7
6	5-$MePhen^+$	−0.78 (−0.87)	0.00	5.0×10^7
	Eth^+	1.46[b] (1.37)[b]		

[a] Values in parentheses were determined in the absence of DNA. [b] One-electron oxidation potential.

direction as the solvent polarity decreases: −0.70 V (H_2O), −0.63 V (MeCN), −0.54 V (CH_2Cl_2), −0.52 V ($CHCl_3$), and −0.42 V (benzene).[20]

In the case of other acridinium, quinolinium, and phenathridinium ions, the E^0_{red} values were determined as the SHACV intersection potentials (Supporting Information, S2).[26] The E^0_{red} values are shifted in a positive direction with increasing DNA concentration in parallel with the absorbance change of intercalators due to intercalation into DNA. The changes in the E^0_{red} values by interaction into DNA are summarized in Table 1. The largest positive potential shift is obtained for $AcrH^+$ (0.19 V) and $CNQuH^+$ (0.19 V) whereas the smallest potential shift is obtained for $AcrCH_2Ph^+$ (0.03 V). This indicates the steric effect of the substituent plays an important role in the stabilization of the intercalator radical due to the $\pi-\pi$ interaction with base pairs of DNA and also in solvation with solvent molecules outside DNA. The binding constant K of $AcrPr^{i+}$ with DNA (2.0×10^3 M^{-1}) is smaller than the K value of $AcrH^+$ (6.7×10^3 M^{-1}) determined by the spectral titration because of the steric effect of the Pr^i group. In any case, the shift in the one-electron reduction potentials of intercalators, which varies depending on the type of intercalators (Table 1), demonstrates that it is essential to determine the E^0_{red} values of intercalators in DNA in order to examine the exact driving force dependence of the photoinduced electron transfer of intercalators.

The one-electron oxidation potential (E^0_{ox}) of Eth^+ is also shifted in a positive direction from 1.37 V in 5 mM Tris-HCl buffer aqueous solution to 1.46 V by interaction into DNA (1.5×10^{-3} M). The positive shift of E^0_{ox} of Eth^+ in DNA indicates that $Eth^{\bullet 2+}$ is less solvated and thereby less stabilized in DNA as compared to that in H_2O. The change in E^0_{ox} of Eth^+ with DNA concentration (Figure 3a) is also in parallel with the number of intercalated Eth^+ ions relative to the initial number of Eth^+ ions, which is determined from a bathchromic shift in the absorption band due to Eth^+ by intercalation into DNA (Figure 3b). In the case of Eth^+, the smaller $[DNA\ bases]_0/[Eth^+]_0$ value is required to complete the change in E^0_{ox} and the absorbance as compared to the case of $AcrPr^{i+}$ in Figure 2. This indicates that the binding of Eth^+ with DNA is stronger than the binding of $AcrPr^{i+}$.

Fluorescence Quenching by Eth^+ via PET in DNA. A drastic enhancement of Eth^+ fluorescence intensity is observed in the presence of DNA as compared to that in its absence.[27] A pathway for the nonradiative decay of excited ethidium in an aqueous solution has been proposed in which the ion donates a proton from one of its amino groups to the solvent.[27] When intercalated into DNA, however, the proton-transfer pathway is virtually eliminated, leading to a lengthening of the singlet excited-state lifetime from 1.8 ns in water to 22 ns and an increase in the fluorescence intensity by about 1 order of magnitude.[28]

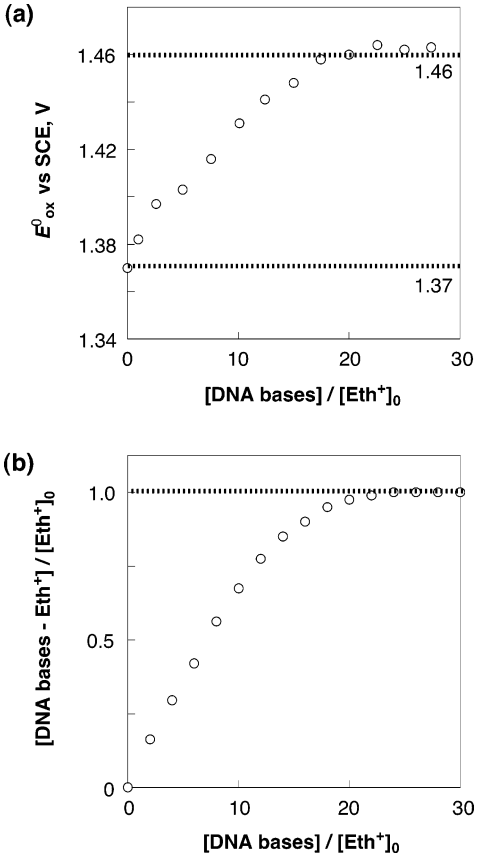

Figure 3. (a) Plot of the one-electron oxidation potential of Eth^+ (5.0×10^{-5} M) vs the ratio of the concentration of DNA ($0-1.5 \times 10^{-3}$ M) to Eth^+ in 5 mM Tris-HCl buffer (pH 7.0), determined by SHACV. (b) Plot of the ratio of intercalated Eth^+ (5.0×10^{-5} M) vs the concentration of DNA ($0-1.5 \times 10^{-3}$ M) to $AcrPr^{i+}$.

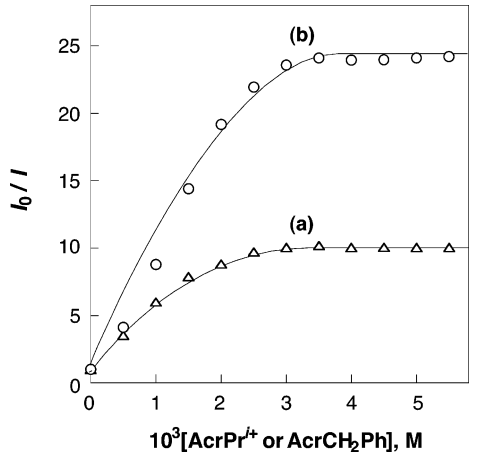

Figure 4. Stern−Volmer plots of the quenching of $^1Eth^{+*}$ (5.0×10^{-5} M) by (a) $AcrPr^{i+}$ ($0-5.5 \times 10^{-3}$ M) and (b) $AcrCH_2Ph$ ($0-5.5 \times 10^{-3}$ M) in the presence of DNA (1.5×10^{-3} M) in 5 mM Tris-HCl buffer (pH 7.0).

The fluorescence of Eth^+ is quenched efficiently by $AcrPr^{i+}$ in the presence of DNA in 5 mM Tris-HCl buffer (pH 7.0) when both Eth^+ and $AcrPr^{i+}$ are intercalated into DNA. The Stern−Volmer plot is shown in Figure 4a, where the I_0/I value increases linearly with increasing $AcrPr^{i+}$ concentration to reach a constant value. Similar results are obtained for $AcrCH_2Ph^+$ (Figure 4b).

From the initial slope and fluorescence lifetime of intercalated Eth^+ (22 ns), the quenching rate constant is obtained as 2.3×10^{11} M^{-1} s^{-1}, which exceeds the limit of the diffusion rate constant significantly. Because the diffusion rate constant of Eth^+ intercalated into DNA is not known, the quenching rate

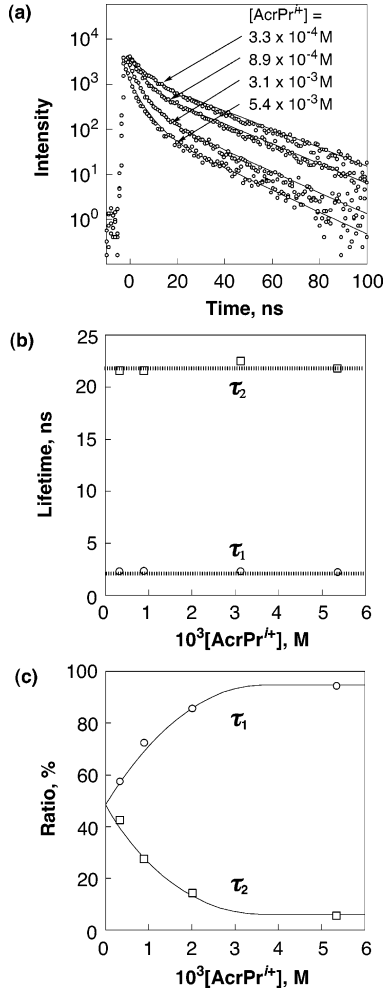

Figure 5. (a) Fluorescence decay curves of Eth^+ (5.0×10^{-5} M) in DNA (1.5×10^{-3} M) in the presence of various concentrations of $AcrPr^{i+}$; $[AcrPr^{i+}] = 3.3 \times 10^{-4}$, 8.9×10^{-4}, 3.1×10^{-3}, and 5.4×10^{-3} M. (b) Plot of two fluorescence lifetimes vs the concentration of $AcrPr^{i+}$. (c) Plot of the component ratio of two fluorescence lifetimes vs the concentration of $AcrPr^{i+}$.

TABLE 2: Quenching Constants (K_q) and Quenching Rate Constants (k_q) of Eth^{+*} by *p*-Benzoquinone Derivatives in the Presence of DNA and the One-Electron Reduction Potentials (E^0_{red}) of Quinone Derivatives

quinone	K_q, M^{-1}	k_q, $M^{-1}\,s^{-1}$	E^0_{red} vs SCE, V
Q	55	2.5×10^9	0.15
Me-Q	50	2.3×10^9	0.14
Cl-Q	66	3.0×10^9	0.15

constants of Eth^+ intercalated into DNA were determined by using strong oxidants such as *p*-benzoquinone (Q) and its derivatives (X−Q; X = Me and Cl), which cannot be intercalated into DNA. The quenching rate constants (k_q) were determined from the slopes of Stern−Volmer plots for the fluorescence quenching of Eth^+ by *p*-benzoquinones in the presence of DNA (Supporting Information S1). The k_q values are listed in Table 2 together with the E^0_{red} values of *p*-benzoquinones, which were also determined by the SHACV method (S2). The k_q values are virtually the same, irrespective of the large difference in the E^0_{red} values. In each case, the free-energy change of electron transfer from Eth^{+*} to *p*-benzoquinones is largely negative, and thereby the k_q values may correspond to the diffusion rate constant of Eth^+ intercalated into DNA.

The k_q value obtained in the fluorescence quenching of Eth^+ by $AcrPr^{i+}$ in the presence of DNA is much larger than the diffusion-limited value, which indicates that fluorescence quenching results from static quenching rather than dynamic quenching. In such a case, the constant I_0/I value in Figure 4 may correspond to the fluorescence quenching of Eth^+ by the nearest-neighbor $AcrR^+$ intercalated into DNA. This is confirmed by the fluorescence lifetime measurements (vide infra).

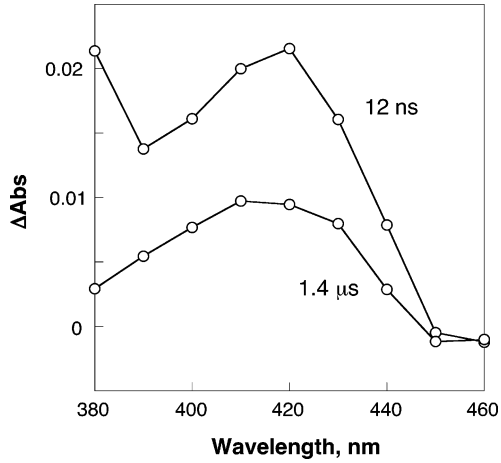

Figure 6. Decay time profiles of absorbance at 420 nm observed by photoexcitation of a 5 mM Tris-HCl buffer (pH 7.0) of Eth^+(2.0×10^{-4} M) with $AcrPr^{i+}$ (2.0×10^{-4} M) in the presence of DNA(3.0×10^{-3} M) obtained after laser excitation at 12 ns and 1.4 μs.

The fluorescence decay dynamics of Eth^+ in the presence of DNA (1.5×10^{-3} M) and $AcrPr^{i+}$ ($3.3 \times 10^{-4} - 5.4 \times 10^{-3}$ M) is shown in Figure 5a. Each decay curve can be well fit with two exponentials. The lifetime of each component (τ_1 and τ_2) is constant irrespective of $AcrPr^{i+}$ concentration as shown in Figure 5b, where the lifetime of the slower component (τ_2 = 22 ns) agrees with the lifetime intercalated into DNA in the absence of $AcrPr^{i+}$ (22 ns). The percentage of the faster component (τ_1) increases with increasing $AcrPr^{i+}$ concentration to reach 100%, whereas the slow component (τ_2) decreases to zero (Figure 5c). The faster component is not ascribed to the replacement of intercalated Eth^+ by $AcrPr^{i+}$ because the absorption band due to intercalated Eth^+ is not affected by the presence of a large excess of $AcrPr^{i+}$ (Supporting Information S3).[29] These results indicate that the singlet excited state ($^1Eth^{+*}$) is quenched by nearest-neighbor $AcrPr^{i+}$ intercalated into DNA. The energy transfer from $^1Eth^{+*}$ to $AcrPr^{i+}$ is unlikely to occur because the singlet excited state of $AcrPr^{i+}$ in DNA (2.89 eV)[30] is significantly higher in energy than that of Eth^+ in DNA (2.24 eV). The ET rate from $^1Eth^{+*}$ to $AcrPr^{i+}$ separated by an additional base pair may be negligible because the ET rate in DNA is known to be sensitive to the donor−acceptor distance.[16b] Although a decay curve analysis using three exponentials is possible, two exponentials are enough to analyze all of the data for different $AcrPr^{i+}$ concentrations.[31] Thus, the rate constant of PET (k_{ET}) from $^1Eth^{+*}$ to $AcrPr^{i+}$ in DNA is determined from the shorter lifetime of $^1Eth^{+*}$ in DNA in the presence of $AcrPr^{i+}$ ($k_{ET} = \tau_1^{-1}$). Similarly, the k_{ET} values of a series of 10-methylacridinium and 1-methylquinolinium ion derivatives were determined as listed in Table 1.[32]

Transient Absorption Spectra in PET in DNA. The fluorescence quenching in Figure 4 occurs via PET from $^1Eth^{+*}$ to $AcrPr^{i+}$ in DNA because $Eth^{\bullet 2+}$ is observed in transient absorption spectra obtained by laser flash photolysis of 5 mM Tris-HCl buffer aqueous solution containing Eth^+, $AcrPr^{i+}$, and DNA with the excitation laser light (λ = 532 nm), which excites only Eth^+ as shown in Figure 6. The transient absorption band observed at 420 nm is assigned to $Eth^{\bullet 2+}$ produced in PET from $^1Eth^{+*}$ to $AcrPr^{i+}$ by comparison with the reported absorption band due to $Eth^{\bullet 2+}$.[11,13] The rise of the transient absorption of

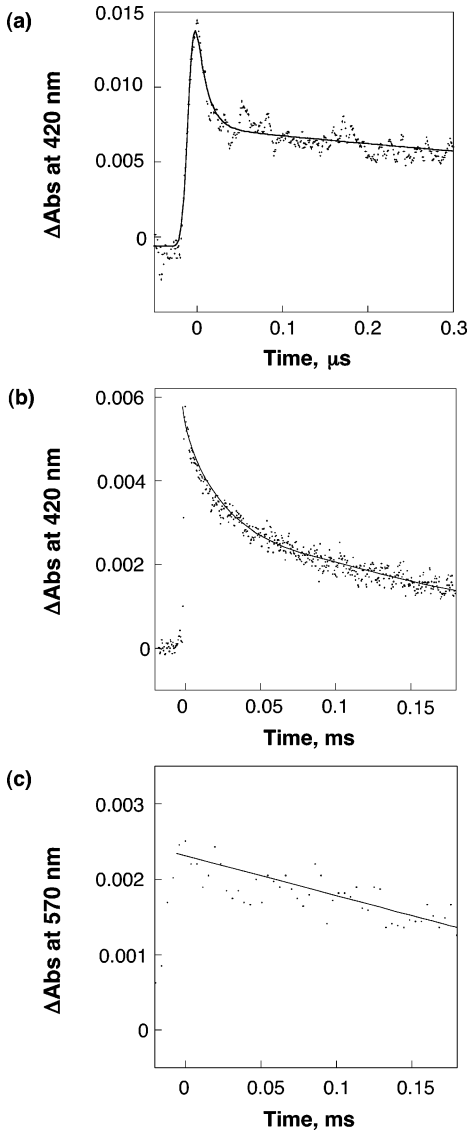

Figure 7. Decay profiles of absorbance at 420 nm (a) in the 100-ns range, (b) in the 100-μs range, and (c) at 570 nm, observed by the photoexcitation of 5 mM Tris-HCl buffer containing $AcrPr^{i+}$ (2.0×10^{-4} M), Eth^{+} (2.0×10^{-4} M), and DNA (6.0×10^{-3} M).

TABLE 3: Lifetime of $Eth^{\bullet 2+}$ in DNA Observed in Photoinduced Electron Transfer from $^1Eth^{+*}$ to Intercalators in 5 mM Tris-HCl Buffer (pH 7.0)

intercalator	τ, ns
$AcrH^{+}$	9
$Acr(CH_2Ph)^{+}$	11
$AcrPr^{i+}$	16
3-$BrQuH^{+}$	13
3-$CNQuH^{+}$	11
5-$MePhen^{+}$	12

$Eth^{\bullet 2+}$ occurs within the instrumental response (10 ns), being consistent with the rate constant (3.9×10^8 s^{-1}) that corresponds to the lifetime ($\tau_1 = 2.3$ ns) in Figure 4a. The absorbance decays rapidly, obeying first-order kinetics to leave residual absorbance (Figure 7a), which decays much more slowly at prolonged reaction time (Figure 7b). Similar results were obtained for other acridinium and quinolinium ion derivatives (Supporting Information S4). The rate constants (k_d) of the initial fast decay are listed in Table 3. The initial fast decay may be attributed to the facile electron transfer from a nucleobase, which interacts with $Eth^{\bullet 2+}$, to $Eth^{\bullet 2+}$ because the k_d values are rather constant irrespective of electron acceptors (Table 3). Only the most oxidizable nucleobase, that is, guanine,[33,34] may be oxidized by $Eth^{\bullet 2+}$. This may be the reason that only a part of the absorbance due to $Eth^{2\bullet +}$ decays rapidly.

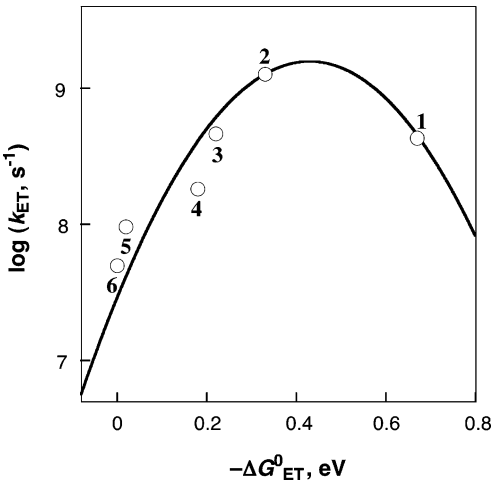

Figure 8. Marcus plot of log k_{ET} vs $-\Delta G^0_{ET}$. Numbers refer to intercalators in Table 1.

Unfortunately, the transient absorption band due to $AcrPr^{i\bullet}$ ($\lambda_{max} = 520$ nm)[20,35] was masked by the excitation light (532 nm). However, the decay of absorbance at 570 nm due to $AcrPr^{i\bullet}$ can be monitored (Figure 7c), and it is much slower than the decay of the longer-lived $Eth^{\bullet 2+}$ (Figure 7b). This indicates that the radical ions generated in the primary PET reaction, $Eth^{\bullet 2+}$ and $AcrPr^{i\bullet}$, recombine by different pathways. $Eth^{\bullet 2+}$ accepts an electron from a nucleobase, which follows by the hole migration to guanine and is accompanied by deprotonation,[36−38] whereas $AcrPr^{i\bullet}$ remains unreacted.[39]

Driving Force Dependence of PET Rates in DNA. The driving force of PET in DNA ($-\Delta G^0_{ET}$) was determined from the E^0_{ox} value of $^1Eth^{+*}$ in DNA (-0.78 V) and the E^0_{red} values of intercalators in DNA, and these values are also listed in Table 1. The determination of both k_{ET} and the driving force in DNA enables us to examine the exact driving force dependence of k_{ET} for PET from $^1Eth^{+*}$ to intercalators in DNA. A plot of log k_{ET} versus $-\Delta G^0_{ET}$ in DNA is shown in Figure 8, where the log k_{ET} value increases when increasing the driving force to reach a maximum and then decreases at a larger driving force. Such a driving force dependence of log k_{ET} in Figure 8 can be analyzed using the Marcus equation of nonadiabatic intramolecular electron transfer (eq 3),

$$k_{ET} = \left(\frac{4\pi^3}{h^2 \lambda k_B T}\right)^{1/2} V^2 \exp\left[-\frac{(\Delta G^0_{ET} + \lambda)^2}{4\lambda k_B T}\right] \qquad (3)$$

where λ is the reorganization energy of photoinduced electron transfer, V is the coupling matrix element, k_B is the Boltzmann constant, h is the Planck constant, and T is the absolute temperature.[40]

The reasonable fit of the data for all of the intercalators to a single Marcus curve affords the values of $\lambda = 0.43$ eV and $V = 2.0$ cm^{-1} (Figure 8).[41] This indicates that differences in the geometry or solvation depending on the investigated intercalators do not have significant effects on the λ and V values. The λ value is similar to the values for PET of the zinc chlorin-C_{60} dyad (0.48 eV)[42] and the zinc porphyrin-C_{60} dyad (0.66 eV)[43] with edge-to-edge distances of 5.89 and 11.9 Å, respectively, that are significantly smaller than the value of the porphyrin-quinone dyad (1.12 eV) with a center-to-center distance of 12.2 Å.[44] However, the V value (2.0 cm^{-1}) is smaller than the value

($6.8\ cm^{-1}$) of the zinc chlorin-C_{60} dyad with an edge-to-edge distance (R_{ee}) of 5.89 Å,[42] which is much smaller than the V value ($230\ cm^{-1}$) reported by Lewis et al.[16b] that is derived from the driving force dependence of the dynamics of PET in hairpin-forming bis(oligonucleotide) conjugates in which the acceptor linker and donor nucleobases are located adjacent to each other. They reported a smaller V value ($17\ cm^{-1}$) for π-stacked bridge-mediated PET in which the acceptor linker and donor nucleobases are separated by two base pairs.[16b] Harriman[5] also reported the V value ($4.4\ cm^{-1}$) for ET between an intercalated donor and acceptor separated by three intervening base pairs. Thus, the distance between Eth^+ and the nearest-neighbor intercalator in DNA may be more than twice the average stacking distance of 3.4 Å. This estimation seems reasonable because the intercalation of two intercalators into adjacent base pairs is unlikely to occur because of the steric repulsion. However, the exact geometry of two intercalated molecules in DNA has yet to be clarified. In any case, the relatively small λ value (0.43 eV) indicates that electron transfer in DNA requires only a small reorganization energy and thus DNA is an ideal environment for efficient electron transfer.

Acknowledgment. This work was partially supported by Grants-in-Aid for Scientific Research on Priority Area (nos. 13440216 and 13031059) from the Ministry of Education, Culture, Sports, Science and Technology, Japan.

Supporting Information Available: Stern−Volmer plots for the fluorescence quenching of Eth^+ by *p*-benzoquinones, SHACV for the reduction of *p*-benzoquinones, the UV−vis spectral change of Eth^+ in DNA in the presence of various concentrations of $AcrPr^{i+}$, and decay time profiles of $Eth^{\bullet 2+}$ in the PET obtained by laser flash photolysis. This material is available free of charge via the Internet at http://pubs.acs.org.

References and Notes

(1) (a) Erkkila, K. E.; Odom, D. T.; Barton, J. K. *Chem. Rev.* **1999**, *99*, 2777. (b) Burrows, C. J.; Muller, J. G. *Chem. Rev.* **1998**, *98*, 1109. (c) Armitage, B. *Chem. Rev.* **1998**, *98*, 1171.

(2) (a) Hall, D. B.; Holmlin, R. E.; Barton, J. K. *Nature* **1996**, *382*, 731. (b) Holmlin, R. E.; Dandliker, P. J.; Barton, J. K. *Angew. Chem., Int. Ed. Engl.* **1997**, *36*, 2714. (c) Nunez, M. E.; Hall, D. B.; Barton, J. K. *Chem. Biol.* **1999**, *6*, 85.

(3) (a) Lewis, F. D.; Wu, T.; Zhang, Y.; Letsinger, R. L.; Greenfiled, S. R.; Wasielewski, M. R. *Science* **1997**, *277*, 673. (b) Lewis, F. D.; Letsinger, R. L.; Wasielewski, M. R. *Acc. Chem. Res.* **2001**, *34*, 159. (c) Lewis, F. D.; Liu, X.; Liu, J.; Miller, S. E.; Hayes, R. T.; Wasielewski, M. R. *Nature* **2000**, *406*, 51. (d) Lewis, F. D. In *Electron Transfer in Chemistry*; Balzani, V., Ed.; Wiley-VCH: Weinheim, Germany, 2001; Vol. 3, pp 105−175.

(4) (a) Giese, B. *Acc. Chem. Res.* **2000**, *33*, 631. (b) Giese, B. *Annu. Rev. Biochem.* **2002**, *71*, 51. (c) Giese, B.; Amaudrut, J.; Kohler, A. K.; Spormann, M.; Wessley, S. *Nature* **2001**, *412*, 318. (d) Meggers, E.; Dussy, A.; Schäfer, T.; Giese, B. *Chem.−Eur. J.* **2000**, *6*, 485.

(5) (a) Harriman, A. *Angew. Chem., Int. Ed.* **1999**, *38*, 945. (b) Grinstaff, M. W. *Angew. Chem., Int. Ed.* **1999**, *38*, 3629. (c) Fukui, K.; Kazuyoshi, T. *Angew. Chem., Int. Ed.* **1998**, *37*, 158. (d) Meade, T. J.; Kayyem, J. F. *Angew. Chem., Int. Ed. Engl.* **1995**, *34*, 352.

(6) (a) Murphy, C. J.; Arkin, M. R.; Ghatlia, N. D.; Bossmann, S.; Turro, N. J.; Barton, J. K. *Proc. Natl. Acad. Sci. U.S.A.* **1994**, *91*, 5315. (b) Arkin, M. R.; Stemp, E. D. A.; Holmlin, R. E.; Barton, J. K.; Hörmann, A.; Olson, E. J. C.; Barbara, P. F. *Science* **1996**, *273*, 475.

(7) Schuster, G. B. *Acc. Chem. Res.* **2000**, *33*, 253.

(8) (a) Gasper, S. M.; Schuster, G. B. *J. Am. Chem. Soc.* **1997**, *119*, 12762. (b) Henderson, P. T.; Jones, D.; Hampikian, G.; Kan, Y.; Schuster, G. B. *Proc. Natl. Acad. Sci. U.S.A.* **1999**, *96*, 8353.

(9) (a) Waring, M. J. *J. Mol. Biol.* **1965**, *13*, 269. (b) LePecq, J. B.; Paoletti, C. *J. Mol. Biol.* **1967**, *27*, 87.

(10) (a) Atherton, S. J.; Beaumont, P. C. *Photobiochem. Photobiophys.* **1984**, *8*, 103. (b) Atherton, S. J.; Beaumont, P. C. *J. Phys. Chem.* **1986**, *90*, 2252. (c) Atherton, S. J.; Beaumont, P. C. *J. Phys. Chem.* **1987**, *91*, 3993.

(11) (a) Brun, A. M.; Harriman, A. *J. Am. Chem. Soc.* **1992**, *114*, 3656. (b) Brun, A. M.; Harriman, A. *J. Am. Chem. Soc.* **1994**, *116*, 10383.

(12) (a) Dandlinker, P. J.; Holmlin, R. E.; Barton, J. K. *Science* **1997**, *275*, 1465. (b) Kelley, S. O.; Holmlin, R. E.; Stemp, E. D. A.; Barton, J. K. *J. Am. Chem. Soc.* **1997**, *119*, 9861. (c) Qu, X.; Chaires, J. B. *J. Am. Chem. Soc.* **1999**, *121*, 2649.

(13) Kononov, A. I.; Moroshkina, E. B.; Tkachenko, N. V.; Lemmetyinen, H. *J. Phys. Chem. B* **2001**, *105*, 535.

(14) (a) Bixon, M.; Jortner, J. *Adv. Chem. Phys.* **1999**, *106*, 35. (b) Jortner, J.; Bixon, M.; Langenbacher, T.; Michel-Beyerie, M. E. *Proc. Natl. Acad. Sci. U.S.A.* **1998**, *95*, 12759.

(15) (a) Kang, Y. K.; Rubtsov, I. V.; Iovine, P. M.; Chen, J.; Therien, M. J. *J. Am. Chem. Soc.* **2002**, *124*, 8275. (b) Grozema, F. C.; Berlin, Y. A.; Siebbeles, L. D. A. *J. Am. Chem. Soc.* **2000**, *122*, 10903.

(16) (a) Lewis, F. D.; Wu, T.; Liu, X.; Letsinger, R. L.; Greenfield, S. R.; Miller, S. E.; Wasielewski, M. R. *J. Am. Chem. Soc.* **2000**, *122*, 2889. (b) Lewis, F. D.; Kalgutkar, R. S.; Wu, Y.; Liu, J.; Hayes, R. T.; Miller, S. E.; Wasielewski, M. R. *J. Am. Chem. Soc.* **2000**, *122*, 12346. (c) Lewis, F. D.; Liu, J.; Weigel, W.; Rettig, W.; Kurnikov, I. V.; Beratan, D. N. *Proc. Natl. Acad. Sci. U.S.A.* **2002**, *99*, 12536.

(17) (a) Anderson, R. F.; Wright, G. A. *Phys. Chem. Chem. Phys.* **1999**, *1*, 4827. (b) Anderson, R. F.; Patel, K. B. *J. Chem. Soc., Faraday Trans.* **1991**, *87*, 3739.

(18) Roberts, R. M. G.; Ostovic, D.; Kreevoy, M. M. *Faraday Discuss. Chem. Soc.* **1982**, *74*, 257.

(19) Fukuzumi, S.; Koumitsu, S.; Hironaka, K.; Tanaka, T. *J. Am. Chem. Soc.* **1987**, *109*, 305.

(20) Fukuzumi, S.; Ohkubo, K.; Tokuda, Y.; Suenobu, T. *J. Am. Chem. Soc.* **2000**, *122*, 4286.

(21) Perrin, D. D.; Armarego, W. L. F.; Perrin, D. R. *Purification of Laboratory Chemicals*, 4th ed.; Pergamon Press: Elmsford, NY, 1996.

(22) Bard, A. J.; Faulkner, L. R. In *Electrochemical Methods: Fundamentals and Applications*; Wiley & Sons: New York, 2001; Chapter 10, pp 368−416.

(23) Mann, C. K.; Barnes, K. K. *Electrochemical Reactions in Nonaqueous Systems*; Marcel Dekker: New York, 1990.

(24) Reichmann, M. E.; Rice, S. A.; Thomas, C. A.; Doty, P. *J. Am. Chem. Soc.* **1954**, *76*, 3047.

(25) The SHACV method provides a superior approach to evaluating directly the one-electron redox potentials in the presence of a follow-up chemical reaction, relative to the better-known dc and fundamental harmonic ac methods: (a) Bond, A. M.; Smith, D. E. *Anal. Chem.* **1974**, *46*, 1946. (b) Arnett, E. M.; Amarnath, K.; Harvey, N. G.; Cheng, J.-P. *J. Am. Chem. Soc.* **1990**, *112*, 344.

(26) The CV gave only irreversible cathodic waves because of the instability of the one-electron reduced species.

(27) Morgan, A. R.; Lee, J. S.; Pulleyblank. D. E.; Murray, N. L.; Evans, D. H. *Nucleic Acids Res.* **1979**, *7*, 547.

(28) (a) Olmstead, J.; Kearns, D. R. *Biochemistry* **1977**, *16*, 3647. (b) Pal, S. K.; Mandal, D.; Bhattaacharyya, K. *J. Phys. Chem. B* **1998**, *102*, 11017.

(29) The loss of fluorescence derived from the displacement of Eth^+ from DNA has been utilized as a high-resolution method for establishing the DNA binding affinity. See Boger, D. L.; Fink, B. E.; Brunette, S. R.; Tse, W. C.; Hedrick, M. P. *J. Am. Chem. Soc.* **2001**, *123*, 5878. In the present case, however, no displacement of Eth^+ by $AcrPr^{i+}$ is observed because of the much stronger binding of Eth^+ than $AcrPr^{i+}$ with DNA.

(30) The singlet excited-state energies of $AcrPr^{i+}$ in the absence and presence of DNA are determined to be 2.72 and 2.89 eV from the absorption maxima (419 and 408 nm) and fluorescence maxima (498 and 453 nm) of $AcrPr^{i+}$ in the absence and presence of DNA, respectively.

(31) Adding the third exponential did not improve the goodness (mean weighted square deviation) of the fit.

(32) The shorter lifetimes of $^1Eth^{+*}$ in DNA in the presence of a series of 10-methylacridinium and 1-methylquinolinium ion derivatives vary depending on their redox potentials. No displacement of Eth^+ by the acridinium and quinolinium derivatives is observed.

(33) (a) Zhu, Q.; LeBreton, P. R. *J. Am. Chem. Soc.* **2000**, *122*, 12824. (b) Kim, N. S.; Zhu, Q.; LeBreton, P. R. *J. Am. Chem. Soc.* **1999**, *121*, 11516.

(34) Sugiyama, H.; Saito, I. *J. Am. Chem. Soc.* **1996**, *118*, 7063.

(35) Fukuzumi, S.; Tanaka, T. *Photoinduced Electron Transfer*; Fox, M. A., Chanon, M., Eds.; Elsevier: Amsterdam, 1988; Part C, p 578.

(36) (a) Candeias, L. P.; O'Neill, P.; Jones, G. D. D.; Steenken, S. *Int. J. Radiat. Biol.* **1992**, *61*, 15. (b) Steenken, S. *Biol. Chem.* **1997**, *378*, 1293.

(37) Weatherly, S. C.; Yang, I. V.; Thorp, H. H. *J. Am. Chem. Soc.* **2001**, *123*, 1236.

(38) Cai, Z.; Gu, Z.; Sevilla, M. D. *J. Phys. Chem. B* **2001**, *105*, 6031.

(39) The absorbance at 570 nm decays at prolonged reaction time probably because of intermolecular dimerization, although the decay mechanism has yet to be clarified.

(40) (a) Marcus, R. A.; Sutin, N. *Biochim. Biophys. Acta* **1985**, *811*, 265. (b) Marcus, R. A. *Angew. Chem., Int. Ed. Engl.* **1993**, *32*, 1111.

(41) In the Marcus classical formalism,[40] nuclear tunneling in the inverted region to excited vibrational states of the acceptor is neglected because it is significant only for highly exergonic ET reactions. See ref 14; Liang, N.; Miller, J. R.; Closs, G. L. *J. Am. Chem. Soc.* **1990**, *112*, 5353.

(42) (a) Fukuzumi, S.; Ohkubo, K.; Imahori, H.; Shao, J.; Ou, Z.; Zheng, G.; Chen, Y.; Pandey, R. K.; Fujitsuka, M.; Ito, O.; Kadish, K. M. *J. Am. Chem. Soc.* **2001**, *123*, 10676. (b) Ohkubo, K.; Imahori, H.; Shao, J.; Ou, Z.; Kadish, K. M.; Chen, Y.; Pandey, R. K.; Fujitsuka, M.; Ito, O.; Fukuzumi, S. *J. Phys. Chem. A* **2002**, *106*, 10991.

(43) Imahori, H.; Tamaki, K.; Guldi, D. M.; Luo, C.; Fujitsuka, M.; Ito, O.; Sakata, Y.; Fukuzumi, S. *J. Am. Chem. Soc.* **2001**, *123*, 2607.

(44) Tsue, H.; Imahori, H.; Kaneda, T.; Tanaka, Y.; Okada, T.; Tamaki, K.; Sakata, Y. *J. Am. Chem. Soc.* **2000**, *122*, 2279.